

A mathematical study on non-linear ordinary differential equation for Magnetohydrodynamic flow of the Darcy-Forchheimer nanofluid

Sathyamoorthy Sivasankari and Vembu Ananthaswamy*

Research Scholar, Research Centre and PG Department of Mathematics, The Madura College (Affiliated to Madurai Kamaraj University), Madurai, Tamil Nadu, India.

Abstract

An analytical study is carried out to obtain the approximate solution for the Magnetohydrodynamic (MHD) flow issue of Darcy-Forchheimer nanofluid containing motile microorganisms having viscous dissipation effect through a non-linear extended sheet employing a new approximate analytical method namely Ananthaswamy-Sivasankari Method (ASM) and also Modified Homotopy Analysis method (MHAM). The derived analytical solution is given in explicit form and is compared with the numerical solution. The graphical results are interlined to reflect the effects of various physical parameters involved in the problem. The numerical computation of the Nusselt number, the local skin friction parameter, and the Sherwood number are compared and shown in the table. Faster convergence is acquired using this strategy. The solution obtained by this method is closer to the exact solution. Also, the solution is in the simplest and most explicit form. It is applicable for all initial and boundary value problems with non-zero boundary conditions. This method can be easily extended to solve other non-linear higher order boundary value problems in physical, chemical, and biological sciences.

Keywords. Darcy-Forchheimer nanofluid flow, Viscous dissipation, Gyrotactic Microorganisms, Ananthaswamy-Sivasankari method (ASM), Modified Homotopy analysis method (MHAM).

2010 Mathematics Subject Classification. 34B40, 34E05, 34E10, 34E15, 34E20.

1. INTRODUCTION

Researchers were highly inspired to investigate the consequences of nanofluid flow as compared to basic fluid flows nowadays. Nanofluid offers a wide range of uses, including heat transfer applications such as electronic cooling systems, radiators, and heat exchangers. The laminar, free convection flow in such an open container employing Lattice Boltzmann method (LBM) with the combination of carbon nanotube and Cu nanoparticles were numerically performed by Choi [10] and he concluded that the Carbon nanotube nanoparticle performs better to boost convection rate than Cu- nanoparticles. The second phase slipping flows of such a nanofluid on a stretching/shrinking sheet deeply embedded in a dynamically layered porous medium with the addition of Ohmic as well as viscous dissipation effects were studied by Ganesh et al. [12].

Darcy-Forchheimer flow changes the temperature distributions by playing a role like an energy source, which leads to affected heat transfer rates. Forchheimer [11] established a square velocity term that is added to the equation of velocity to illustrate the imprints of boundaries and inertia. This is what Muskat [22] referred to as the "Forchheimer term," which is suitable for high Reynolds numbers. Forchheimer [11] explained the flow of such an incompressible fluid with variable fluid viscosity and changeable thermal conductivity using thermal radiation, Dufour and Soret as well as heat and mass transfer across a linearly rotating porous vertical semi-infinite plate having suction and solved with the use of the shooting method with Runge-Kutta fourth-order method and Newton-Raphson's interpolation scheme. Sadiq et al. [26] analyzed the Darcy-Forchheimer movement in magneto Maxwell fluid along a convectively heated surface. Saif et al. [27] evaluated the Darcy-Forchheimer flow for nanofluid caused by a curved extended

Received: 08 February 2023 ; Accepted: 22 April 2023.

* Corresponding author. Email: ananthu9777@gmail.com.

surface. The influence of viscous dissipation for both assisting and opposing flows and thermophoresis onto a blended convection fluid of Darcy- Forchheimer within a soaked porous media was explained in Seddeek [29]. More applications of the Darcy-Forchheimer flow can be found in [30–32].

In the work of Muhammad et al. [21], the Magnetohydrodynamic (MHD) elongated motion of Maxwell nanofluid containing non-linear porous medium and convective temperature impacts was solved using Homotopy analysis technique analytically. The analysis of the Magnetohydrodynamic (MHD) extended flows of Maxwell nanofluid involving the convective boundary condition with the consideration of some notable physical factors such as activation energy, radiative heat flux and dynamic thermal conductivity were studied by Sajid et al. [28]. For further information on the peculiarities for the flow of Magnetohydrodynamic Darcy-Forchheimer nanofluid via a non-linear stretching sheet, see Rasool et al. [24]. A numerical investigation was conducted on the Magnetohydrodynamic (MHD) Williamson nanofluid flow enabled to move over a porous medium that is separated from it by a flat surface that is non-linearly extending and the second rule of thermodynamics was applied to analyze the fluid motion, energy, and temperature transport including the components of entropy generation utilizing the Buongiorno model by Rasool et al. [25].

With the help of numerical methods, many problems have been evaluated easily in physical sciences. Akhter et al. [3] described the irreversibility research study of steady flow including the magnetic forces among two infinitely stretched discs located within a Darcy-Forchheimer medium. With the use of similarity transformations the dimensionless formulation of the regulating equations was solved by the quasi linearization technique numerically. Ali et al. [4] study the connection of the thermally and hydrodynamically formed flows over a vertical square duct only with the magnetic field created with a located near wire, under the temperature boundary condition having uniform heat flux over the unit axial length using the finite volume technique. Zakullah et al. [37] examined the numerical solution for the Darcy-Forchheimer 3D flow of nanofluid through a rotating surface with thermal generation/absorption. The numerical study of the Darcy-Forchheimer flows for nanofluid induced on an exponentially extending curved surface was addressed in Hayat et al. [14]. Turk et al. [35] provided the finite element method (FEM) answer for the natural convection flows of micro polar nanofluids under the influence on an auxiliary magnetic field.

Analytical methods give more accurate results as compared to numerical methods. There are many analytical methods which provide an approximate solution for non-linear problems. Hayat et al. [13] established the convergence series solution through the Optimal Homotopy Analysis method (OHAM) for three-dimensional flow of Williamson nanoliquid over a non-linear stretchable surface with Darcy-Forchheimer porous medium fluid flow and he considered the effects of thermophoresis and Brownian diffusion. Khan et al. [15] focused on three-dimensional micro polar Darcy-Forchheimer nanofluid flow of water (H_2O) based carbon nanotubes (CNTs). Nanofluid flow was simulated in a moving system along with thermally transmitting flow of micropolar nanofluid and the governing equations were resolved through HAM. The expression of Darcy-Forchheimer thin fluid flows of SWCNT-water nanoliquid and corresponding heat transfer issue over an unstable stretching plate in two-dimensional using HAM was demonstrated by Nasir et al. [23]. In [5–7], HAM is used in a wide variety of applications.

Ahmed et al. [1] investigated a comprehensive analysis of motile microorganisms and activation energy in the flow of pure as well as hybrid nanoliquids subject to Darcy-Forchheimer medium and reported that the use of the porous medium not only stables the flow but also maintains the thermal characteristics of the fluid. Ahmed et al. [2] considered the mass and thermal transport flow from moving gyrotactic microorganisms (microbes) with solid nanoparticles in the viscous dissipation effect, and indeed the flow model PDEs were numerically handled with the SOR (successive over relaxation) technique. Shahid et al. [31] derived the solution of the characteristics of blood circulation carrying gyrotactic microorganisms forced with a capillary comprising stretching medium and permeable throughout the existence of a magnetic field via the aid of successive Taylor series linearization method (STSLM). Sohail et al. [34] presented the entropy analysis of three-dimensional Maxwell nanofluid containing gyrotactic microorganism under the phenomenon of thermal and energy transport with Cattaneo-Christov theory along with homogeneous-heterogeneous reactions over a linear stretched surface. The bio-convection flow of Williamson nanofluid through a funnel in the midst of motile gyrotactic microorganism was investigated by Waqas et al. [36].

As a consequence from the aforementioned articles, we have concentrated on the implications of such viscous dissipation upon the Magnetohydrodynamic (MHD) Darcy-Forchheimer flow of nanoliquid containing gyrotactic microorganisms. The objective of this investigation is to provide the approximate solution of the considered non-linear



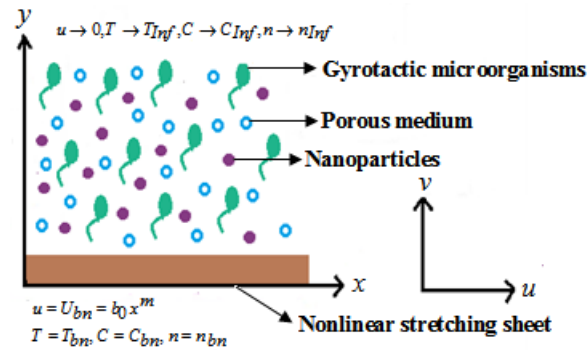


FIGURE 1. Flow Diagram.

problem analytically in the closed and explicit manner after converting dimensionless equations. The computed results are then compared with the numerical solution. The impacts of various physical parameters are graphically presented.

2. MATHEMATICAL FORMULATION OF THE PROBLEM

Let us have a view at the persistent viscous, two-dimensional, unsteady Magnetohydrodynamic (MHD) Darcy-Forchheimer flow of the nanofluid caused by an extending sheet that exhibits non-linear behavior, as reported by Batool et al. [8]. The sheet continues to move along the x -axis with only a stretching speed of type $U_{bn} = b_0 x^m$, where m and $b_0 > 0$ are constant relative terms. The flow problem's configuration is presented in Figure 1.

The current flow problem is described by the following system of differential equations

$$\frac{\partial u}{\partial x} + \frac{\partial v}{\partial y} = 0, \quad (2.1)$$

$$u \frac{\partial u}{\partial x} + v \frac{\partial v}{\partial y} = v \left(\frac{\partial^2 u}{\partial y^2} \right) - \left(\frac{\sigma_{Ec} B_0^2 x^{m-1}}{\rho_{Fl}} + \frac{v}{K_*} \right) u - \frac{c_B}{\sqrt{K_*}} u^2, \quad (2.2)$$

$$u \frac{\partial T}{\partial x} + v \frac{\partial T}{\partial y} = \alpha \frac{\partial^2 T}{\partial y^2} + \frac{(\rho c)_{NP}}{(\rho c)_{Fl}} \times \left[D_{Bm} \left(\frac{\partial C}{\partial y} \frac{\partial T}{\partial y} \right) + \frac{D_{Tp}}{T_{Inf}} \left(\frac{\partial T}{\partial y} \right)^2 \right] + \frac{v}{c_p} \left(\frac{\partial u}{\partial y} \right)^2, \quad (2.3)$$

$$u \frac{\partial C}{\partial x} + v \frac{\partial C}{\partial y} = D_{Bm} \frac{\partial^2 u}{\partial y^2} + \frac{D_{Tp}}{T_{Inf}} \frac{\partial^2 T}{\partial y^2}, \quad (2.4)$$

$$u \frac{\partial n}{\partial x} + v \frac{\partial n}{\partial y} + \frac{b_{ch} W_{cs}}{(C_{bn} - C_{Inf})} \left[\frac{\partial}{\partial y} \left(n \frac{\partial C}{\partial y} \right) \right] = D_{Gm} \frac{\partial^2 n}{\partial y^2}. \quad (2.5)$$

The boundary conditions for the aforementioned equations are:

$$u = U_{bn} = b_0 x^m, \quad v = 0, \quad T = T_{bn}, \quad C = C_{bn}, \quad n = n_{bn} \quad \text{at } y = 0, \quad (2.6)$$

$$u \rightarrow 0, \quad T \rightarrow T_{Inf}, \quad C \rightarrow C_{Inf}, \quad n \rightarrow n_{Inf} \quad \text{as } y \rightarrow \infty. \quad (2.7)$$

Now let us define the dimensionless quantities

$$\eta = \frac{1}{2} \sqrt{\frac{2b_0(m+1)\rho_{Fl}}{\mu}} x^{\frac{m-1}{2}} y, \quad \theta(\eta) = \frac{T - T_{Inf}}{T_{bn} - T_{Inf}}, \quad \chi(\eta) = \frac{n - n_{Inf}}{n_{bn} - n_{Inf}},$$

$$\phi(\eta) = \frac{C - C_{Inf}}{C_{bn} - C_{Inf}}, \quad u = b_0 x^m f'(\eta), \quad v = -\frac{1}{2} \sqrt{2b_0(m+1)} v x^{\frac{m-1}{2}}. \quad (2.8)$$

The velocity components $u = \frac{\partial \psi}{\partial y}$ and $v = -\frac{\partial \psi}{\partial x}$ help to construct a stream function ψ and η serve as a symbol for the dimensionless similarity variable. The elements u and v contribute to Eq. (2.1) in the form of ψ . The transformation



mentioned in Eq. (2.8) can be used to generate Eqs. (2.2) – (2.5) into the following ODE’s:

$$f''' + ff'' - \left[\frac{2m}{m+1} \right] f'^2 - Me^2 f' - \lambda f' - Fr(f')^2 = 0, \tag{2.9}$$

$$\theta'' + Pr [Nb\theta'\phi' + Nt\theta'^2 + \theta'f] + PrEc f'^2 = 0, \tag{2.10}$$

$$\phi'' + \frac{Nt}{Nb} \theta'' + LePr(f'\phi') = 0, \tag{2.11}$$

$$\chi'' Sc(f\chi') - Pe[\chi'\phi' + \phi''(\chi + \sigma)] = 0. \tag{2.12}$$

The dimensionless form of boundary conditions specified in Eqs. (2.6) and (2.7) is given by

$$f(0) = 0, f'(0) = 1, \theta(0) = 1, \phi(0) = 1, \chi(0) = 1 \text{ at } \eta = 0, \tag{2.13}$$

$$f'(\infty) \rightarrow 0, \theta(\infty) \rightarrow 0, \phi(\infty) \rightarrow 0, \chi(\infty) \rightarrow 0 \text{ as } \eta \rightarrow \infty, \tag{2.14}$$

where primes symbolize derivatives with respect to η . Moreover, Me is a magnetic parameter, Nt is a thermophoresis parameter, Nb is a parameter of Brownian motion, Le is a Lewis number, λ is a porosity parameter, Ec denotes a Eckert number, Pr is a Prandtl number, Sc is a Schmidt number, Pe indicates a Peclet number, σ_{Ec} is a constant term and Fr is the Forchheimer parameter which has the following mathematical forms:

$$Nt = \frac{(\rho c)_{Np} D_{Th} (T_{bn} - T_{Inf})}{(\rho c)_{Fl} v T_{Inf}}, Nb = \frac{(\rho c)_{Np} D_{Bm} (C_{bn} - C_{Inf})}{(\rho c)_{Fl} v}, Pr = \frac{v}{\alpha},$$

$$Ec = \frac{(u_{bn})^2}{c_p (T_{bn} - T_{Inf})}, Sc = \frac{v}{D_{Gm}}, Le = \frac{v}{D_{Bm}}, Me = \sqrt{\frac{2\sigma_{Ec} B_0^2}{b_0 \rho_{Fl} (m+1)}},$$

$$Pe = \frac{b_{ch} W_{cs}}{D_{Gm}}, \sigma_{Ec} = \frac{n_{Inf}}{(n_{bn} - n_{Inf})}, \lambda = \frac{2v}{K_* b_0 (m+1) x^{m-1}}, Fr = \frac{2c_b x}{k_*^{1/2} (m+1)}. \tag{2.15}$$

3. APPROXIMATE ANALYTICAL SOLUTION USING ASM AND MHAM

For the purpose of estimating the third-order non-linear ordinary differential equations, a new technique known as the Ananthaswamy-Sivasankari method (ASM) [9, 33] is introduced. One can use it to resolve both linear as well as non-linear differential equations. It is also simple to adapt this approach to deal with some other non-linear such boundary value issues in physical, chemical, and biological sciences, especially for MHD flow problems in physical science. However, the proposed new method is applicable to problems involving initial and boundary values. Additional boundary conditions can be produced for the differential equation and its derivatives. It’s really simple to understand and apply the technique. The solution contains only three arbitrary constants which depend upon the order of the differential equation and it is easy to find the values of these arbitrary constants. If we can apply HAM, HPM, NHPM, ADM, and VIM, it will be take two or more iterations but this method takes a single iteration which contains all the parameters involved in the equation. The error percentage will be less than 0.3% when comparing the proposed method with the exact solution/numerical simulation/numerical solution. In Appendix-A, the basic concept of ASM is explained.

Many different difficulties in science and engineering have been resolved effectively using the Homotopy analysis method. It is a non-perturbative analytical method for getting series solutions to non-linear equations. HAM provides the ability to modify and regulate the convergence of a solution via the so-called convergence-control parameter in comparison to other perturbative and non-perturbative analytical methods. This has leading to HAM emerging as the most efficient technique for deriving analytical solutions in terms of the unknown function and its derivatives. Previous applications of HAM have primarily concentrated on non-linear differential equations for which the non-linearity is such a polynomial in the work of Liao [16–20]. For non-linear issues, Liao [16–20] created the Homotopy analysis approach, which is an effective analytical method. It offers an analytical solution in terms of an infinite power series. However, it is necessary in practice to assess this result and get numerical values using the infinite power series. The entire system of differential equations was solved to examine the precision with the Homotopy analysis technique (HAM) solution with a finite number of terms. We have a simple mechanism to control and modify the convergence domain of the



solution series owing to the auxiliary parameter, which is a component in the homotopy analysis approach. The basic concept of MHAM is provided in Appendix-B.

The results obtained for the non-dimensional velocity, temperature, concentration, and density distributions are provided below along with their analytical derivation.

3.1. Approximate Analytical solution of Velocity distribution using ASM [9, 33]. The following is the approximate analytical solution for the velocity distribution in Eq. (2.9) which satisfies the following boundary conditions

$$f(\eta) = l + qe^{a\eta} + re^{-a\eta}, \quad (3.1)$$

$$f'(\eta) = aqe^{a\eta} - are^{-a\eta}. \quad (3.2)$$

Utilizing the boundary conditions in Eqs. (2.13) and (2.14), we determine the value for the parameters $l, q,$ and r as follows:

$$l = \frac{1}{a}, \quad q = 0, \quad r = -\frac{1}{a}. \quad (3.3)$$

Thus, the Eq. (3.1) becomes

$$f(\eta) = \frac{1}{a} - \frac{1}{a}e^{-a\eta}. \quad (3.4)$$

Now, by using the Eq. (3.4) into Eq. (2.9) and on simplification, we get

$$a^2e^{-a\eta} + \left[\left(\frac{1}{a} - \frac{1}{a}e^{-a\eta} \right) (-ae^{-a\eta}) \right] - \left[\frac{2m}{m+1} \right] e^{-2a\eta} - Me^2e^{-a\eta} - \lambda e^{-a\eta} - Fr e^{-2a\eta} = 0. \quad (3.5)$$

Now, taking $\eta = 0$, Eq. (3.5) becomes

$$a^2 - \left(\frac{2}{m+1} \right) - Me^2 - \lambda - Fr = 0. \quad (3.6)$$

On solving the Eq. (3.6), we get the value of the parameter a , which is given by

$$a = \pm \sqrt{\left(\frac{2}{m+1} \right) + Me^2 + \lambda + Fr}. \quad (3.7)$$

Hence, an approximate analytical solution for the velocity distribution is found by inserting an Eq. (3.7) into Eq. (3.1) as follows:

$$f(\eta) = \frac{1}{a} - \frac{1}{a}e^{-a\eta}, \quad (3.8)$$

where a is obtained in Eq. (3.7).

3.2. Approximate analytical solution of temperature, concentration and density distribution using MHAM [5–7]. After substituting an Eq. (3.8) into the Eqs. (2.10), (2.11), and (2.12), we get the following transformed temperature, concentration, and density distribution equations

$$\theta'' + Pr \left[Nb\theta'\phi' + Nt\theta'^2 + \theta' \left(\frac{1}{a} - \frac{1}{a}e^{-a\eta} \right) \right] + PrEc (a^2e^{-2a\eta}) = 0, \quad (3.9)$$

$$\phi'' + \frac{Nt}{Nb}\theta'' + LePr (e^{-a\eta}\phi') = 0, \quad (3.10)$$

$$\chi'' + Sc \left[\left(\frac{1}{a} - \frac{1}{a}e^{-a\eta} \right) \chi' \right] - Pe [\chi'\phi' + \phi''(\chi + \sigma)] = 0. \quad (3.11)$$



We generate the following Homotopy for the Eqs. (3.9), (3.10), and (3.11) as

$$(1 - p)\theta'' = hp \left(\theta'' + Pr \left[Nb\theta'\phi' + Nt\theta'^2 + \theta' \left(\frac{1}{a} - \frac{1}{a}e^{-a\eta} \right) \right] + PrEc(a^2e^{-2a\eta}) \right), \tag{3.12}$$

$$(1 - p)\phi'' = hp \left(\phi'' + \frac{Nt}{Nb}\theta'' + LePr(e^{-a\eta}\phi') \right), \tag{3.13}$$

$$(1 - p)\chi'' = hp \left(\chi'' + Sc \left[\left(\frac{1}{a} - \frac{1}{a}e^{-a\eta} \right) \chi' \right] - Pe[\chi'\phi' + \phi''(\chi + \sigma)] \right). \tag{3.14}$$

The initial approximation for Eqs. (3.12) to (3.14) is provided by

$$\theta_0(0) = 1, \theta_0(\infty) \rightarrow 0 \text{ and } \theta_i(0) = 0, \theta_i(\infty) \rightarrow 0, i = 1, 2, 3, \dots, \tag{3.15}$$

$$\phi_0(0) = 1, \phi_0(\infty) \rightarrow 0 \text{ and } \phi_i(0) = 0, \phi_i(\infty) \rightarrow 0, i = 1, 2, 3, \dots, \tag{3.16}$$

$$\chi_0(0) = 1, \chi_0(\infty) \rightarrow 0 \text{ and } \chi_i(0) = 0, \chi_i(\infty) \rightarrow 0, i = 1, 2, 3, \dots \tag{3.17}$$

The approximate analytical solutions to the Eqs. (3.9) to (3.12) are:

$$\theta = \theta_0 + p\theta_1 + p^2\theta_2 + \dots, \tag{3.18}$$

$$\phi = \phi_0 + p\phi_1 + p^2\phi_2 + \dots, \tag{3.19}$$

$$\chi = \chi_0 + p\chi_1 + p^2\chi_2 + \dots \tag{3.20}$$

Substituting the Eqs. (3.18) to (3.20) into the Eqs. (3.12) to (3.14) respectively and comparing the coefficients of like powers of p , we acquire the following equations

$$p^0 : \theta''_0 = 0, \tag{3.21}$$

$$p^1 : \theta''_1 - \theta''_0 = h \left(\theta''_0 + Pr \left[Nb\theta'_0\phi'_0 + Nt\theta_0'^2 + \theta'_0 \left(\frac{1}{a} - \frac{1}{a}e^{-a\eta} \right) \right] + PrEc(a^2e^{-2a\eta}) \right), \tag{3.22}$$

$$p^0 : \phi''_0 = 0, \tag{3.23}$$

$$p^1 : \phi''_1 - \phi''_0 = h \left(\phi''_0 + \frac{Nt}{Nb}\theta''_0 + LePr(e^{-a\eta}\phi'_0) \right), \tag{3.24}$$

$$p^0 : \chi''_0 = 0, \tag{3.25}$$

$$p^1 : \chi''_1 - \chi''_0 = h \left(\chi''_0 + Sc \left[\left(\frac{1}{a} - \frac{1}{a}e^{-a\eta} \right) \chi'_0 \right] - Pe[\chi'_0\phi'_0 + \phi''_0(\chi_0 + \sigma)] \right). \tag{3.26}$$

In this stage, by using MHAM, the initial guessing solutions for the Eqs. (3.9) to (3.11) which satisfies the boundary conditions in Eqs. (3.15) to (3.17) are:

$$\theta_0(\eta) = e^{-\eta}, \tag{3.27}$$

$$\phi_0(\eta) = e^{-\eta}, \tag{3.28}$$

$$\chi_0(\eta) = e^{-\eta}. \tag{3.29}$$



On solving the Eqs. (3.22), (3.24), and (3.26) with the use of Eqs. (3.27) to (3.29) and utilizing the boundary conditions in Eqs. (3.15) to (3.17), we get the following results

$$\begin{aligned} \theta_1(\eta) = & - \left(h + 1 - \frac{h}{a} + \frac{hPr(Nb + Nt)}{4} + \frac{hPr}{a(1+a)^2} + \frac{hPrEc}{4} \right) e^{-\eta} + \left(h + 1 - \frac{h}{a} \right) e^{-\eta} \\ & + \frac{hPr(Nb + Nt)}{4} e^{-2\eta} + \frac{hPr}{a(1+a)^2} e^{-(1+a)\eta} + \frac{hPrEc}{4} e^{-2a\eta}, \end{aligned} \quad (3.30)$$

$$\phi_1(\eta) = - \left(h + 1 + h \frac{Nt}{Nb} - \frac{hLePr}{(1+a)^2} \right) e^{-\eta} + \left(h + 1 + h \frac{Nt}{Nb} \right) e^{-\eta} - \frac{hLePr}{(1+a)^2} e^{-(1+a)\eta}, \quad (3.31)$$

$$\begin{aligned} \chi_1(\eta) = & - \left(h + 1 - \frac{hSc}{a} - hPe\sigma + \frac{hSc}{a(1+a)^2} - \frac{2hPe}{4} \right) e^{-\eta} + \left(h + 1 - \frac{hSc}{a} - hPe\sigma \right) e^{-\eta} \\ & + \frac{hSc}{a(1+a)^2} e^{-(1+a)\eta} - \frac{2hPe}{4} e^{-2\eta}. \end{aligned} \quad (3.32)$$

According to the HAM technique, we have

$$\theta = \lim_{p \rightarrow 1} \theta(\eta) = \theta_0 + \theta_1, \quad (3.33)$$

$$\phi = \lim_{p \rightarrow 1} \phi(\eta) = \phi_0 + \phi_1, \quad (3.34)$$

$$\chi = \lim_{p \rightarrow 1} \chi(\eta) = \chi_0 + \chi_1. \quad (3.35)$$

Hence, the approximate analytical solutions of the temperature, concentration, and density distribution equations are obtained by substituting the Eqs. (3.27) to (3.32) into the Eqs. (3.33) to (3.35) respectively, as follows

$$\begin{aligned} \theta(\eta) = & e^{-\eta} - \left(h + 1 - \frac{h}{a} + \frac{hPr(Nb + Nt)}{4} + \frac{hPr}{a(1+a)^2} + \frac{hPrEc}{4} \right) e^{-\eta} + \left(h + 1 - \frac{h}{a} \right) e^{-\eta} \\ & + \frac{hPr(Nb + Nt)}{4} e^{-2\eta} + \frac{hPr}{a(1+a)^2} e^{-(1+a)\eta} + \frac{hPrEc}{4} e^{-2a\eta}, \end{aligned} \quad (3.36)$$

$$\phi(\eta) = e^{-\eta} - \left(h + 1 + h \frac{Nt}{Nb} - \frac{hLePr}{(1+a)^2} \right) e^{-\eta} + \left(h + 1 + h \frac{Nt}{Nb} \right) e^{-\eta} - \frac{hLePr}{(1+a)^2} e^{-(1+a)\eta}, \quad (3.37)$$

$$\begin{aligned} \chi(\eta) = & e^{-\eta} - \left(h + 1 - \frac{hSc}{a} - hPe\sigma + \frac{hSc}{a(1+a)^2} - \frac{2hPe}{4} \right) e^{-\eta} + \left(h + 1 - \frac{hSc}{a} - hPe\sigma \right) e^{-\eta} \\ & + \frac{hSc}{a(1+a)^2} e^{-(1+a)\eta} - \frac{2hPe}{4} e^{-2\eta}. \end{aligned} \quad (3.38)$$

4. RESULTS AND DISCUSSION

In this section, we have discussed the impacts of several physical parameters involved in this flow problem. Also, we have displayed a comparison between the analytical solution obtained in Eqs. (3.8), (3.36), (3.37), and (3.38) of dimensionless velocity, temperature, concentration and density distribution respectively with the numerical results using Successive Over Relaxation (SOR) method described in [8].

Figures 2 to 13 represent the comparison of analytical results and numerical results for dimensionless velocity, temperature, concentration and density distribution respectively with various values of the physical parameters such as the Magnetic parameter Me , Parameter of Brownian motion Nb , porosity parameter λ , Lewis number Le , Prandtl number Pr , Schmidt number Sc , Parameter of thermophoresis Nt , Peclet number Pe , Eckert number Ec , Forchheimer parameter Fr , and Electric conductivity σ_{Ec} .

Figures 2 to 4 show the comparison on the dimensionless velocity using Eq. (3.8) with the numerical result presented in [8] for varying values of Me , λ and Fr . From Figure 2, it is observed that by raising the value of the Magnetic parameter Me , the velocity decreases. According to Figure 3, it is depicted that by increasing the value of the porosity parameter λ , the velocity decreases. As in Figure 4, the velocity decreased by increasing the amount of the Forchheimer



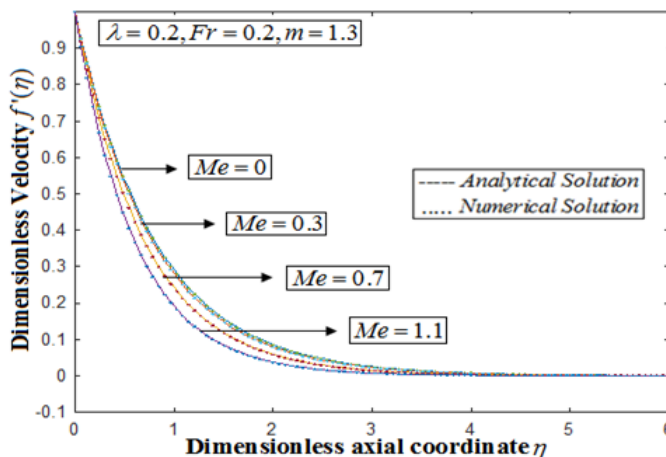


FIGURE 2. The dimensionless velocity with the dimensionless axial coordinate η for some specified values of λ, Fr, m and varying amounts of Me .

parameter Fr . Also, Table 1 clearly evaluated the analytical and numerical results of the velocity $f''(0)$ for several values of the physical quantities Me, λ and Fr .

Figures 5 to 7 interline the comparison with the dimensionless temperature using Eq. (3.36) and numerical result presented in [8] for varying values of Me, λ and Fr . Figure 5 illustrates that the temperature rises by increasing the value of the Magnetic parameter Me . From Figure 6, it is noted that by raising the amount of the porosity parameter λ , the temperature increases. According to Figure 7, the temperature increased by increasing the value of the Forchheimer parameter fr . Table 2 shows the analytical and numerical results of the temperature $-\theta'(0)$ for different amounts of the physical parameters Nt, Nb, λ, Fr, Ec , and Me .

Figures 8 to 10 illustrate the comparison between both the dimensionless concentration using Eq. (3.37) and numerical result presented in [8] for several amounts of Me, λ , and Fr . Figure 8 depicts that the concentration rises by raising the value of the magnetic parameter Me . Also, from Figure 9, it is understood that by increasing the amount of the porosity parameter λ , the concentration increases. From Figure 10, the concentration increased by raising the value of the Forchheimer parameter Fr . Table 3 shows the analytical and numerical results of the concentration $-\phi'(0)$ for changing values of the physical parameters Nt, Nb, λ, Fr, Le and Me .

Figures 11 to 13 demonstrate the comparison on the dimensionless density using Eq. (3.38) with the numerical result presented in [8] for the several values of Me, λ , and Fr . According to Figure 11, it is clearly noted that by raising the amount of the Magnetic parameter Me , the density increases. From Figure 12, indicates that by raising the value of the porosity parameter λ , the density increases. In Figure 13, the density increased by raising the amount of the Forchheimer parameter Fr .

The following significant observations are highlighted from the results:

- As the values of magnetic, porosity and Forchheimer parameters increase, the velocity drops.
- The temperature, microorganism’s concentration, and microorganism’s density increase by raising the value of magnetic, porosity and Forchheimer parameters.

CONCLUSION

The Magnetohydrodynamic (MHD) flow issue of Darcy-Forchheimer nanoliquid including motile microorganisms having viscous dissipation effect over a non-linear extended sheet was examined analytically. The approximate solution was derived using a new approximate analytical method Ananthaswamy-Sivasankari Method (ASM) and Modified Homotopy Analysis Method (MHAM) analytically. The achieved analytical result was reported in explicit form and compared to the numerical solution. The influence of many physical parameters involved in the problem was displayed graphically. Nusselt number, local skin friction coefficient, and also Sherwood number were estimated and shown



TABLE 1. Comparison of analytical and numerical solution for the local skin friction coefficient $f''(0)$ with varying amounts of the parameters λ, Me and Pr .

λ	Me	Pr	Numerical $f''(0)$	Analytical $f''(0)$	Error %
0	0.2	0.9	-1.423938	-1.423643	0.020721
0.3	0.2	0.9	-1.53581	-1.535885	0.004883
0.5	0.2	0.9	-1.606089	-1.606745	0.040828
0.2	0	0.9	-1.423938	-1.423539	0.028029
0.2	0.2	0.9	-1.499455	-1.499047	0.027217
0.2	0.4	0.9	-1.571352	-1.571460	0.006873
0.2	0.2	0	-1.267705	-1.253437	1.138310
0.2	0.2	0.3	-1.349067	-1.348903	0.012158
0.2	0.2	0.6	-1.426118	-1.426025	0.006522
Average error percentage					0.142838

TABLE 2. Comparison of both analytical and numerical solutions for the Nusselt number $-\theta'(0)$ for numerous amounts of the parameters λ, Me, Nb, Nt, Fr and Ec .

Nt	Nb	λ	Fr	Ec	Me	Numerical $-\theta'(0)$	Analytical $-\theta'(0)$	Error %
0.1	0.2	0.2	0.9	0.1	0.2	0.445417	0.445879	0.103616
0.2	0.2	0.2	0.9	0.1	0.2	0.415899	0.415912	0.003126
0.4	0.2	0.2	0.9	0.1	0.2	0.385252	0.386140	0.229968
0.1	0.1	0.2	0.9	0.1	0.2	0.467118	0.469900	0.592041
0.1	0.2	0.2	0.9	0.1	0.2	0.432433	0.432522	0.020577
0.1	0.4	0.2	0.9	0.1	0.2	0.391482	0.391985	0.128321
0.1	0.2	0.0	0.9	0.1	0.2	0.456385	0.457368	0.214925
0.1	0.2	0.3	0.9	0.1	0.2	0.426793	0.436887	2.310437
0.1	0.2	0.5	0.9	0.1	0.2	0.414351	0.416361	0.482754
0.1	0.2	0.2	0.0	0.1	0.2	0.466133	0.466471	0.072459
0.1	0.2	0.2	0.3	0.1	0.2	0.446389	0.446509	0.026875
0.1	0.2	0.2	0.6	0.1	0.2	0.437961	0.438139	0.040626
0.1	0.2	0.2	0.9	0.0	0.2	0.499539	0.499686	0.029418
0.1	0.2	0.2	0.9	0.1	0.2	0.431806	0.431826	0.004632
0.1	0.2	0.2	0.9	0.2	0.2	0.376081	0.376606	0.139403
0.1	0.2	0.2	0.9	0.1	0.0	0.456385	0.456456	0.015555
0.1	0.2	0.2	0.9	0.1	0.2	0.432169	0.433079	0.210123
0.1	0.2	0.2	0.9	0.1	0.4	0.419783	0.419877	0.022388
Average error percentage								0.258180



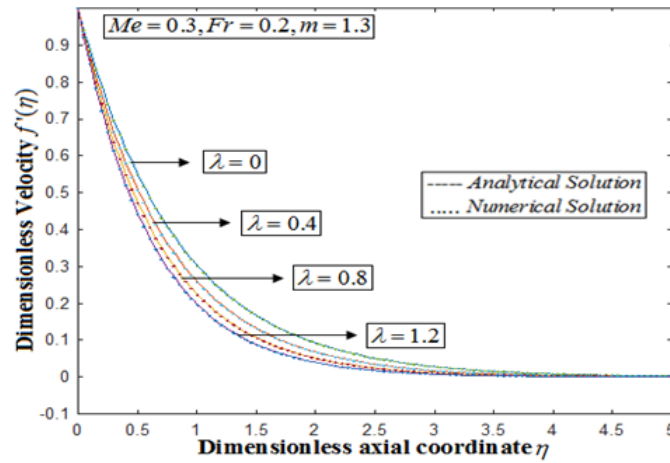


FIGURE 3. The dimensionless velocity with the dimensionless axial coordinate η for varying values of λ and certain fixed values of Me, Fr, m .

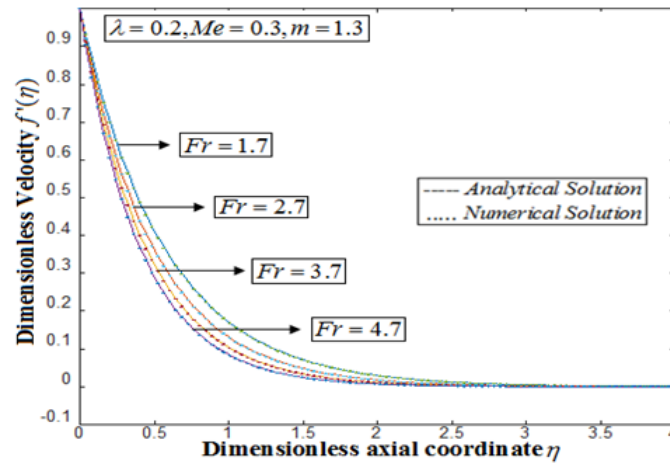


FIGURE 4. The dimensionless velocity with the dimensionless axial coordinate η in some fixed amounts of λ, Me, m and distinct values of Fr .

in the table. The overall absolute error percentage is less than 0.3%, when comparing the analytical solution with the numerical solution. It is not ensured that this method is applicable to partial differential equations. It is not guaranteed that this method is closer to the exact/numerical solution/numerical simulation when the given ODE has zero boundary conditions.



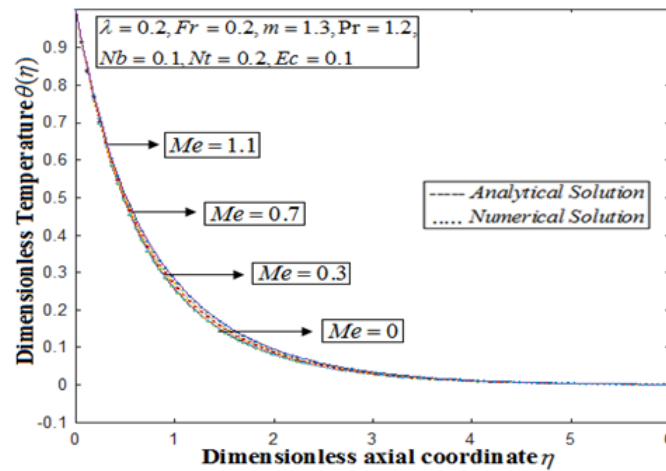


FIGURE 5. The dimensionless temperature with the dimensionless axial coordinate η for distinct values of Me and in some particular amounts of λ , Fr , Nb , Nt , Pr , m and Ec .

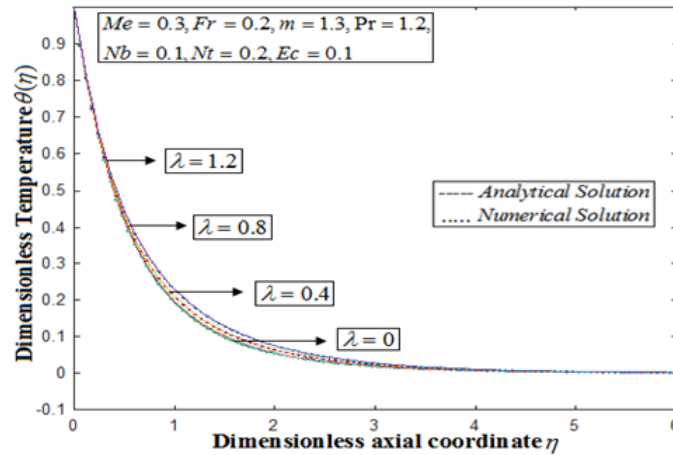


FIGURE 6. The dimensionless temperature with the dimensionless axial coordinate η for different amounts of λ and particular values of Me , Fr , Nb , Nt , Pr , m and Ec .



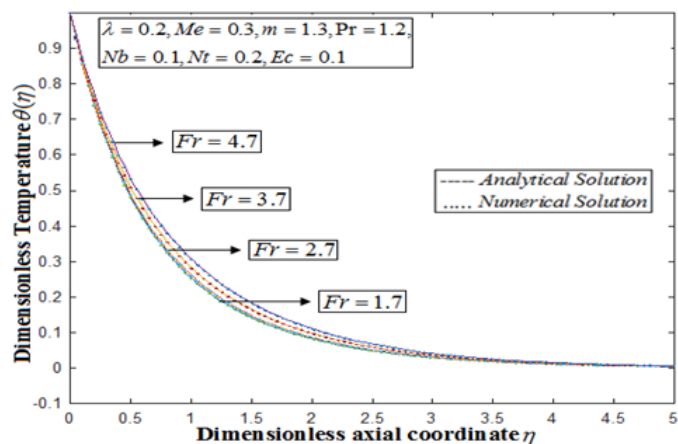


FIGURE 7. The dimensionless temperature with the dimensionless axial coordinate η for several amounts of Fr and in some constant values of $Me, \lambda, Nb, Nt, Pr, m$ and Ec .

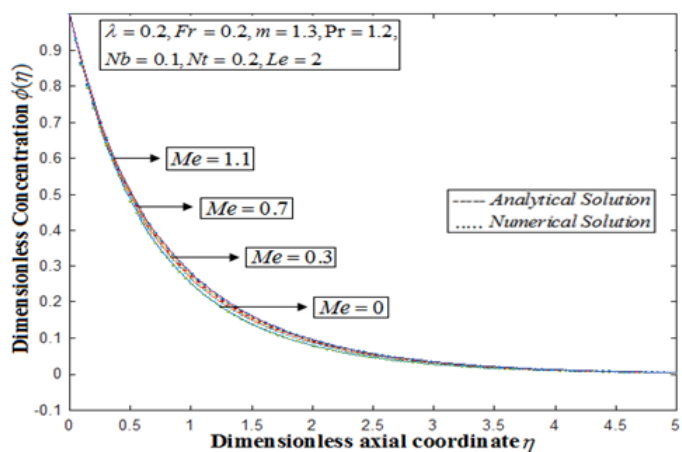


FIGURE 8. The dimensionless concentration with the dimensionless axial coordinate η including varying values of Me and some constant amounts of $\lambda, Fr, Nb, Nt, Pr, m$ and Le .



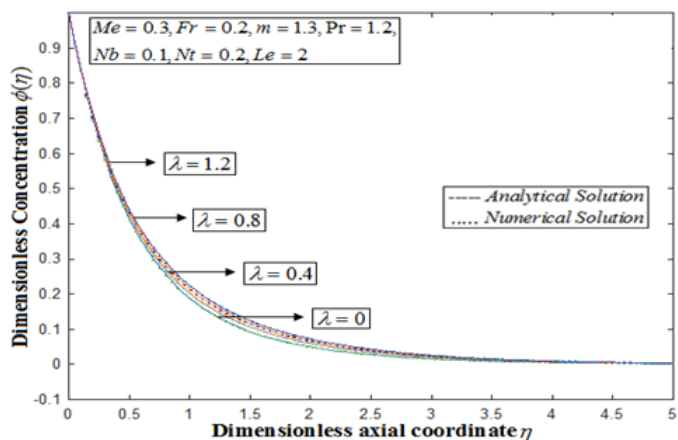


FIGURE 9. The dimensionless concentration with the dimensionless axial coordinate η for distinct amounts of λ and certain fixed values of Me, Fr, Nb, Nr, Pr, m and Le .

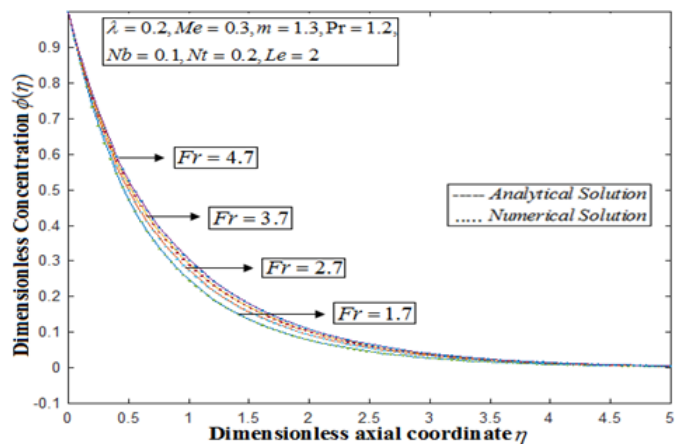


FIGURE 10. The dimensionless concentration with the dimensionless axial coordinate η involving different amounts of Fr and particular amounts of $Me, \lambda, Nb, Nr, Pr, m$ and Le .



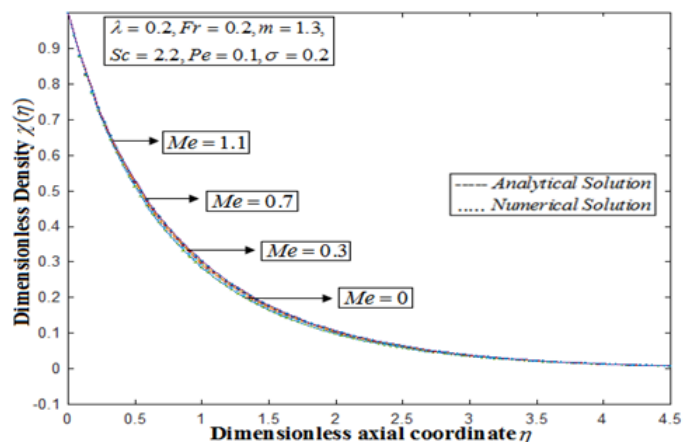


FIGURE 11. The dimensionless density with the dimensionless axial coordinate η considering some constant amounts of $\lambda, Fr, Sc, Pe, m, \sigma$ and distinct values of Me .

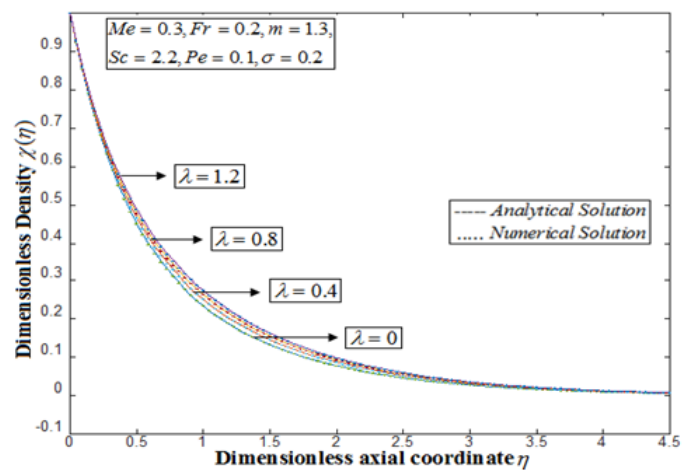


FIGURE 12. The dimensionless density with the dimensionless axial coordinate η in particular values of $Me, Fr, Sc, Pe, m, \sigma$ and varying values of λ .



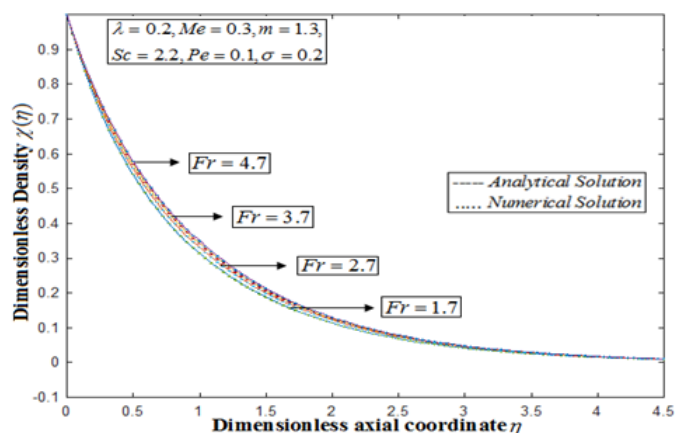


FIGURE 13. The dimensionless density with the dimensionless axial coordinate η assuming certain fixed values of $Me, \lambda, Sc, Pe, m, \sigma$ and different amounts of Fr .

TABLE 3. Comparison with analytical and numerical findings for the Sherwood number $-\phi'(0)$ with several values of the parameters λ, Me, Le, Nb, Nt and Fr .

Me	λ	Le	Nb	Nt	Fr	Numerical $-\phi'(0)$	Analytical $-\phi'(0)$	Error %
0.0	0.2	0.8	0.2	0.1	0.9	0.430925	0.431092	0.038739
0.2	0.2	0.8	0.2	0.1	0.9	0.401441	0.401925	0.120420
0.4	0.2	0.8	0.2	0.1	0.9	0.397490	0.397872	0.096011
0.2	0.0	0.8	0.2	0.1	0.9	0.430925	0.431075	0.034797
0.2	0.3	0.8	0.2	0.1	0.9	0.400779	0.400781	0.000499
0.2	0.5	0.8	0.2	0.1	0.9	0.396747	0.396773	0.006553
0.2	0.2	0.3	0.2	0.1	0.9	0.307160	0.307202	0.013672
0.2	0.2	0.5	0.2	0.1	0.9	0.311506	0.311593	0.027921
0.2	0.2	0.7	0.2	0.1	0.9	0.363977	0.364009	0.008791
0.2	0.2	0.8	0.1	0.1	0.9	0.328577	0.328798	0.067215
0.2	0.2	0.8	0.2	0.1	0.9	0.392125	0.392282	0.040022
0.2	0.2	0.8	0.4	0.1	0.9	0.447677	0.447635	0.009383
0.1	0.2	0.8	0.2	0.1	0.9	0.429622	0.429705	0.019316
0.1	0.2	0.8	0.2	0.2	0.9	0.335406	0.335479	0.021760
0.1	0.2	0.8	0.2	0.4	0.9	0.237252	0.237311	0.024862
0.2	0.2	0.8	0.7	0.1	0.0	0.431477	0.431434	0.009966
0.2	0.2	0.8	0.7	0.1	0.3	0.402987	0.402998	0.002730
0.2	0.2	0.8	0.7	0.1	0.6	0.399828	0.399853	0.006252
Average error percentage								0.030495



APPENDIX

Appendix A: Basic Concept of Ananthaswamy-Sivasankari Method [9, 33]. Let us consider the non-linear boundary value problem

$$q : f(y, y', y'', y''') = 0, \tag{A. 1}$$

where q represents the third order non-linear differential equation such that $y = y(x, c, d, \dots)$ in which c, d are given parameters and $x \in [L, U]$ can be finite or infinite considering the associated boundary conditions:

$$\left. \begin{aligned} \text{At } x = L, \quad y(x) = y_{L_0} \quad (\text{or}) \quad y'(x) = y_{L_1} \quad (\text{or}) \quad y''(x) = y_{L_2} \\ \text{At } x = U, \quad y(x) = y_{U_0} \quad (\text{or}) \quad y'(x) = y_{U_1} \quad (\text{or}) \quad y''(x) = y_{U_2} \end{aligned} \right\} \tag{A. 2}$$

Assume that the approximate analytical solution for the non-linear equations is an exponential function of the form

$$y(x) = l + me^{ax} + ne^{-ax}. \tag{A. 3}$$

By resolving the following non-linear differential equations, the unknown coefficients l, m and n are discovered:

$$\left. \begin{aligned} y(L) = l + me^{aL} + ne^{-aL} &= y_{L_0} \\ y'(L) = ame^{aL} - ane^{-aL} &= y_{L_1} \\ y''(L) = a^2me^{aL} + a^2ne^{-aL} &= y_{L_2} \end{aligned} \right\} \tag{A. 4}$$

$$\left. \begin{aligned} y(U) = le^{aU} + me^{-aU} &= y_{U_0} \\ y'(U) = ale^{aU} - ame^{-aU} &= y_{U_1} \\ y''(U) = a^2le^{aU} + a^2me^{-aU} &= y_{U_2} \end{aligned} \right\} \tag{A. 5}$$

The unknown parameters l, m and n may be computed using Eqs. (A. 4) and (A. 5).

The following non-linear differential equations are formed by substituting an Eq. (A. 3) into Eq. (A. 1).

$$q : f(y(x, l, m, n, a, c, d), y'(x, l, m, n, a, c, d), y''(x, l, m, n, a, c, d), y'''(x, l, m, n, a, c, d)) = 0. \tag{A. 6}$$

This equation holds true at x , where $x \in [L, U]$. By resolving Eq. (A. 6), the unknown parameter a can be identified in terms of the existing parameters c and d .

Appendix B: Basic Concept of Modified Homotopy Analysis Method. Consider the differential equation stated below:

$$N[u(t)] = 0, \tag{B. 1}$$

where N represents the non-linear operator, t indicates an independent variable and $u(t)$ refers to an unknown function. For the sake of simplicity, we disregard all boundaries or initial conditions that could be handled similarly. By means of generalizing the conventional Homotopy technique, Liao produced the so-called zero-order deformation equation as follows:

$$(1 - p)L[\phi(t; p) - u_0(t)] = phH(t)(N[\phi(t; p)]), \tag{B. 2}$$

where $p \in [0, 1]$ denotes the embedding parameter, $h \neq 0$ refers to a non-zero auxiliary parameter, and $h \in [-1, 1]$, $H(t) \neq 0$ is an auxiliary function, L is an auxiliary linear operator, $u_0(t)$ specifies an initial guess of $u(t)$, $\phi(t; p)$, is an unknown function. It is essential to note that one has a lot of choices in selecting auxiliary unknowns in HAM. Obviously, when $p = 0$ and $p = 1$, it holds:

$$\phi(t; 0) = u_0(t) \quad \phi(t; 1) = u(t), \tag{B. 3}$$

respectively. Thus as p increases from 0 to 1, the solution $\phi(t; p)$ varies from the initial guess $u_0(t)$ to the solution $u(t)$. Expanding $\phi(t; p)$ in the Taylor series with respect to p , we have:

$$\phi(t; p) = u_0(t) + \sum_{m=1}^{+\infty} u_m(t)p^m, \tag{B. 4}$$



where

$$u_m(t) = \frac{1}{m!} \frac{\partial^m \phi(t; p)}{\partial p^m} \Big|_{p=0}. \quad (\text{B. 5})$$

If the auxiliary linear operator, the initial guess, the auxiliary parameter h , and the auxiliary function are so properly chosen, the series (B. 4) converges at $p = 1$ then we have

$$u(t) = u_0(t) + \sum_{m=1}^{+\infty} u_m(t). \quad (\text{B. 6})$$

Differentiating (B. 2) for m times with respect to the embedding parameter p , and then setting $p = 0$. Finally, dividing them by $m!$, we will have the so-called m^{th} -order deformation equation as follows:

$$L[u_m - K_m u_{m-1}] = hH(t)R_m(u_{m-1}), \quad (\text{B. 7})$$

where

$$R_m(u_{m-1}) = \frac{1}{(m-1)!} \frac{\partial^{m-1}(N[\phi(t; p)])}{\partial p^{m-1}} \Big|_{p=0}, \quad (\text{B. 8})$$

and

$$K_m = \begin{cases} 0, & m \leq 1, \\ n, & \text{otherwise.} \end{cases} \quad (\text{B. 9})$$

Applying L^{-1} on both sides of the Eq. (B. 7), we have

$$u_m(t) = K_m u_{m-1}(t) + hL^{-1}[H(t)R_m(u_{m-1})]. \quad (\text{B. 10})$$

In such a manner, it is simple to attain u_m for $m \geq 1$ at m^{th} order as follows:

$$u(t) = \sum_{m=0}^M u_m(t). \quad (\text{B. 11})$$

When $M \rightarrow +\infty$, we attain an accurate approximation of the original Eq. (B. 1). We suggest Liao [16–20] for more information on the convergence of the aforementioned approach. If Eq. (B. 1) affords a unique solution, then this approach will yield it.

Appendix C: Nomenclature.

CONFLICT OF INTERESTS

The authors declare that there is no conflict of interests.

ACKNOWLEDGMENT

The authors are very grateful to the reviewers for carefully reading the paper and for their comments and suggestions which have improved the paper.



symbol	Meaning
u	x -Component of velocity
v	y -Component of velocity
ρ_{Fl}	Fluid's density
ρ_{Np}	Nanoparticles' density
μ	Dynamic viscosity
ν	Kinematic viscosity
T	Temperature
b_0	Positive constant
c_P	Specific heat
K_*	Permeability of medium
c_B	Drag force coefficient
D_{Bm}	Brownian coefficient
D_{Tp}	Thermophoresis diffusion coefficient
D_{Gm}	Microorganism diffusion coefficient
σ_{Ec}	Electric conductivity
b_{ch}	Chemotaxis constant
W_{cs}	Maximum swimming speed of cell
T_{Inf}	Ambient temperature
T_{bn}	Temperature at surface of sheet
α	Thermal diffusivity
B_c	Strength of magnetic field
Ec	Eckert number
n	Microorganisms' concentration
C	Volume fraction of nanoparticles
Pr	Prandtl number
Me	Magnetic parameter
Sc	Schmidt number
Le	Lewis number
Pe	Peclet number
Nt	Parameter of thermophoresis
Nb	Parameter of Brownian motion
η	Dimensionless variable
λ	Porosity parameter
Fr	Forchheimer parameter

REFERENCES

- [1] S. Ahmad, S. Akhter, M. I. Shahid, K. Ali, M. Akhtar, and M. Ashraf, *Novel thermal aspects of hybrid nanofluid flow comprising of manganese zinc ferrite $MnZnFe_2O_4$, nickel zinc ferrite $NiZnFe_2O_4$ and motile microorganisms*, Ain Shams Eng. J., 13(5) (2022).
- [2] S. Ahmad, J. Younis, K. Ali, M. Rizwan, M. Ashraf and M. A. Abd El Salam, *Impact of swimming gyrotactic microorganisms and viscous dissipation on nanoparticles flow through a permeable medium- a numerical assessment*, J. Nanomater., (2022).
- [3] S. Akhter, S. Ahmad, and M. Ashraf, *Cumulative impact of viscous dissipation and heat generation on MHD Darcy-Forchheimer flow between two stretchable disks: Quasi linearization technique*, J. Sci. Arts., 22(1) (2022), 219–232.



- [4] K. Ali, S. Ahmad, O. Baluch, W. Jamshed, M. R. Eid, and A. A. Pasha, *Numerical study of magnetic field interaction with fully developed flow in a vertical duct*, Alex. Eng. J., *61*(12) (2022), 11351–11363.
- [5] V. Ananthaswamy, C. Sumathi, and M. Subha, *Mathematical analysis of variable viscosity fluid flow through a channel and Homotopy Analysis Method*, Int. J. Mod. Math. Sci., *14*(3) (2016), 296–316.
- [6] V. Ananthaswamy, M. Subha, and A. Mohammed Fathima, *Approximate analytical expression of non-linear boundary value problem for a boundary layer flow using Homotopy Analysis Method*, Madridge J. Bioinform. Syst. Biol., *1*(2) (2019), 34–39.
- [7] V. Ananthaswamy, T. Nithya, and V. K. Santhi, *Mathematical analysis of the Navier- stokes equations for steady Magnetohydrodynamic flow*, J. Inf. Comput. Sci., *10*(3) (2020), 989–1003.
- [8] M. Batool, S. Akhter, S. Ahmad, M. Ashraf, and K. Ali, *Impact of viscous dissipation on MHD Darcy-Forchheimer nanoliquid flow comprising gyrotactic microorganisms past a non-linear extending surface*, Sci. Iran., (2022).
- [9] J. Chitra, V. Ananthaswamy, S. Sivasankari, and Seenith Sivasundaram, *A new approximate analytical method (ASM) for solving non-linear boundary value problem in heat transfer through porous fin*, Math. Eng. Sci. Aerosp. (MESA), *14*(1) (2023), 53–69.
- [10] S. U. S. Choi, *Enhancing thermal conductivity of fluids with nanoparticles developments and application of non-Newtonian flows*, ASME J. Heat Transfer, *66* (1997), 99–105.
- [11] P. Forchheimer, *Wasserbewegung durch Boden*, Zeitschrift des Vereins Deutscher Ingenieure, *45* (1901), 1782–1788.
- [12] N. V. Ganesh, A. K. A. Hakeem, and B. Ganga, *Darcy-Forchheimer flow of hydro magnetic nanofluid over a stretching/shrinking sheet in a thermally stratified porous medium with second order slip, viscous and Ohmic dissipation effects*, Ain Shams Eng. J., *9* (2018), 939–951.
- [13] T. Hayat, A. Aziz, T. Muhammad, and A. Alsaedi, *Darcy-Forchheimer three-dimensional flow of nanofluid over a convectively non-linear stretching surface*, Commun. Theor. Phys., *68*(3) (2017), 387.
- [14] T. Hayat, F. Haider, and T. Muhammad, *Numerical study for Darcy-Forchheimer flow of nanofluid due to an exponentially stretching curved surface*, Results Phys., *8* (2018), 764–771.
- [15] A. Khan, Z. Shah, S. Islam, A. Dawar, E. Bonyah, H. Ullah, and A. Khan, *Darcy-Forchheimer flow of MHD CNTs nanofluid radiative thermal behavior and convective non-uniform heat source/sink in the rotating frame with microstructure and inertial characteristics*, AIP Adv., *8* (2018).
- [16] S. J. Liao, *Proposed homotopy analysis techniques for the solution of non-linear Problems*, Ph.D. dissertation, Shanghai Jiao Tong University, Shanghai (1992).
- [17] S. J. Liao, *An approximate solution technique which does not depend upon small parameters: a special example*, Int. J. Non-Linear Mech., *30* (1995), 371–380.
- [18] S. J. Liao, *A uniformly valid analytic solution of 2D viscous flow past a semi-infinite flat plate*, J. Fluid Mech., *385* (1999), 101–128.
- [19] S. J. Liao, *An explicit totally analytic approximation of Blasius viscous flow problem*, Int. J. Non-Linear Mech., *385* (1999), 385.
- [20] S. J. Liao, *A Analytic solutions of the temperature distribution in blasius viscous flow problems*, J. Fluid Mech., *453* (2019), 411–425.
- [21] T. Muhammad, A. Alsaedi, S. A. Shehzad and T. Hayat, *A revised model for Darcy-Forchheimer flow of Maxwell nanofluid subject to convective boundary condition*, Chinese J. Phys., *55* (2017), 963–976.
- [22] M. Muskat, *The flow of homogenous fluids through porous media*, MI: Edwards, (1995).
- [23] S. Nasir, Z. Shah, S. Islam, E. Bonyah and T. Gul, *Darcy-Forchheimer nanofluid thin film flow of SWCNTs and heat transfer analysis over an unsteady stretching sheet*, AIP Adv., *9* (2019).
- [24] G. Rasool, A. Shafiq, C. M. Khalique, and T. Zhang, *MHD Darcy-Forchheimer nanofluid flow over a non-linear stretching sheet*, Phys. Scr., *94*(10) (2014).
- [25] G. Rasool, T. Zhang, A. J. Chamka, A. Shafiq, I. Tlili, and G. Shahzadi, *Entropy generation and consequences of binary chemical reaction on MHD Darcy-Forchheimer Williamson nanofluid flow over non-linearly stretching surface*, Entropy, *22* (2020).
- [26] M. A. Sadiq and T. Hayat, *Darcy-Forchheimer flow of magneto Maxwell liquid bounded by convectively heated sheet*, Results Phys., *6* (2016), 884–890.



- [27] R. S. Saif, T. Hayat, R. Ellahi, T. Muhammad, and A. Alsaedi, *Darcy-Forchheimer flow of nanofluid due to a curved stretching surface*, *Int. J. Numer. Methods Heat Fluid Flow*, 29 (2019), 2–20.
- [28] T. Sajid, M. Sagheer, S. Hussain, and M. Bilal, *Darcy-Forchheimer flow of Maxwell nanofluid with non-linear thermal radiation and activation energy*, *AIP Adv*, 8 (2018).
- [29] M. A. Seddeek, *Influence of viscous dissipation and thermophoresis on Darcy- Forchheimer mixed convection fluid in a saturated porous media*, *J. Colloid. Interface Sci.*, 293 (2006), 137–142.
- [30] A. Shafiq, G. Rasool, and C. M. Khaliq, *Significance of thermal slip and convective boundary conditions in three-dimensional rotating Darcy-Forchheimer nanofluid flow*, *Symmetry*, 12 (2020).
- [31] A. Shahid, Z. Zhou, M. Hassan, et al., *Computational study of magnetized blood flow in the presence of gyrotactic microorganisms propelled through a permeable capillary in a stretching motion*, *Int. J. Multiscale Comput. Eng.*, 16 (2018), 409–426.
- [32] M. I. Shahid, S. Ahmad, and M. Ashraf, *Simulation analysis of mass and heat transfer attributes in nanoparticles flow subject to Darcy-Forchheimer medium*, *Sci. Iran.*, (2022).
- [33] S. Sivasankari, V. Anantahswamy, and S. Sivasundaram, *A new approximate analytical method for solving some non-linear initial value problems in physical sciences*, *Math. Eng. Sci. Aerosp. (MESA)*, 14(1) (2023), 145–162.
- [34] M. Sohail and R. Naz, *On the onset of entropy generation for a nanofluid with thermal radiation and gyrotactic microorganisms through three-dimensional flows*, *Phys. Scr.*, 95 (2020).
- [35] O. Turk and M. T. Sezin, *TFEM solution to natural convection flow of a micro polar nanofluid in the presence of a magnetic field*, *Meccanica.*, 52 (2017), 889–901.
- [36] H. Waqas, S. U. Khan, M. Imran, and M. Bhatti, *Thermally developed Falkner-Skan bioconvection flow of a magnetized nanofluid in the presence of a motile gyrotactic microorganism: Buongiorno’s nanofluid model*, *Phys. Scr.*, 94 (2019).
- [37] M. Zakaullah, S. S. Capinno, and D. Baleanu, *A numerical simulation for Darcy-Forchheimer flow of nanofluid by a rotating disk with partial slip effects*, *Front. Phys.*, 7 (2020).

